THE STRUCTURE OF THE ŌTAGIRI DOME IN THE RYŌKE METAMORPHIC BELT, CENTRAL JAPAN ——WITH SPECIAL REFERENCE TO THE PETROFABRIC ANALYSIS——

by

Takamura TSUCHIYA

(With 49 Text-Figures and 2 Plates)

Contributions from the Department of Geology and Mineralogy, Faculty of Science, Hokkaidō University. No. 968

Contents

Introduction

The Ōtagiri region is situated in the eastern skirt of Mt. Kisokoma which occupies the northern part of the Central Alps of Japan. The region lies in the northern extremity of the Ryōke metamorphic belt of Central Japan, showing wide

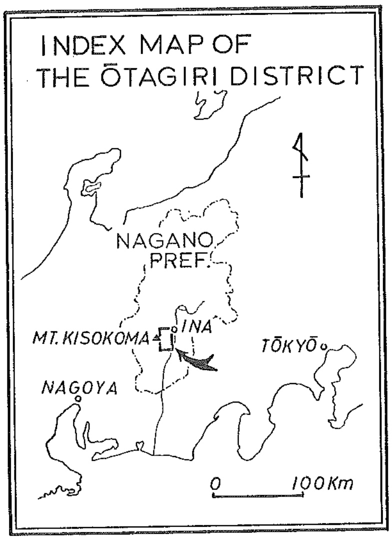

(Index map)

distribution of various kinds of the metamorphic rocks and plutonic rocks. The metamorphic rocks mainly consist of banded gneisses, schistose hornfelses and biotite slates, most of which form a kind of fire-ball shaped dome associated with fine-grained two-mica granite in the centre. It is named the Ōtagiri dome by the present author after the name of the Ōtagiri river which traverses its middle part.

In this article, the structural features of the dome are described from the macro-fabric as well as microfabric points of view.

Since the geological map " Kiso " on the scale of 1: 200,000 was published by NODA (1912), petrological study of the region has been ignored for long time, and it was only in recent years that geological surveys were made, with fruitful results. These papers, however, dealt with mainly from the petrographical and petrological points of view, the tectonic aspect of this region was reported only by KATADA et al. (1961).

The petrofabric investigation in other regions of the Ryōke metamorphic belt has been made by OKAMURA (1960) and NUREKI (1960) in the Yanai region, and also by HARA (1962) in the Kasagi region, both in the southwestern Japan. KANISAWA (1962) carried out a structural analysis in the Takatō region to the east of the present area. The geological structure of the Hiraoka region to the south of the present region was clarified by the Plutonism Research Group of Hokkaidō University (1965a, b,).

The author has divided the region into four subareas and has intended chiefly to establish the tectonic sequence of the Ōtagiri dome accompanied with the intrusion of fine-grained two-mica granites, namely the Ōtagiri granites. For this purpose, megascopical structural analysis of each subarea and microscopical petrofabric analysis were carried out, and the results obtained were compared with the other regions in the Ryōke metamorphic belt.

General geology

MURAYAMA and KATADA (1957) divided the metamorphic rocks in the region into four zones according to the grades of progressive metamorphism as follows:

(1) Zone of biotite slate, (2) zone of schistose hornfels I, (3) zone of schistose hornfels II and (4) zone of banded gneiss, with metamorphic grades increasing from northwest to southeast.

The zone of biotite slate which represents the lowest metamorphic grade makes a gradual transition to the non-metamorphosed, so-called Chichibu Paleozoic System in the north and northwestern region. Most of metamorphic rocks are derived from arenaceous and argillaceous sediments.

ŌKI (1958) added (5) zone of cordierite hornfels which represents a polymetamorphosed zone caused by the intrusion of the Kisokoma granodiorite. This zone is distributed with 1—1.5 km width surrounding the western side of the dome.

The large portion of the dome is occupied by banded gneisses and its northern and western wings are formed by the lower grade metamorphic rocks; schistose hornfels I and schistose hornfels II. In the western extremity they pass into the cordierite hornfelses.

The Ōtagiri granites are classified into two facies from their occurrence and rock types; the gray coloured normal facies and leucocratic aplitic facies. The former intrudes concordantly or nearly concordantly into the country rocks, while the latter intrudes discordantly through the country rocks and the gray normal facies of granites. Since it seems that the former is more closely related with the metamorphism and the up-doming of the Ōtagiri dome, it is treated mainly in the present paper.

The Ōtagiri granites intrude with various shapes from place to place in the main part of the dome, in which two conspicuous masses are recognized, i.e., one is near the centre of the dome and the other in its northwestern wing just traversing its structure. The granite near the centre is an irregular-shaped large mass surrounded by numerous sheets and dykes of various sizes. The other exhibits rather strange sheet-like shape with branches extending only to the southern side. Further many sheets and dykes are distributed only in the southern part of the granite. It stretches from northeast to southwest with a convexity towards the northwest, and is wedged between the northwestern wing and the main part of the dome.

Such feature was explained as the result of its intrusion along the Ōtagiri fault (MURAYAMA and KATADA, 1957, KATADA et al., 1961). The present author considers the Ōtagiri fault took place as a tectonic boundary fault, that is, the discontinuous zone between the granite-gneiss zone (" inner " zone according to KATADA et al., 1961) and the outer zone of KATADA et al. (1961). There is a good evidence that the northwestern boundary of this Ōtagiri granite is comparatively simple and straight, in contrast to its southeastern boundary which is more irregular and complex. Many sheets and dykes are found only in this side. Further an evidence may also be added that the Ōtagiri granite along the Ōtagiri fault shows clastic texture as compared with that of the other.

The Ōtagiri dome extends a long tail to the south, showing a fire-ball shape as a whole. In the western wing of the " head " part it contacts with the Kisokoma granodiorite which represents the post-kinematic granite of the Ryōke plutonism, and in the eastern wing it is overlain by the diluvial gravel beds of the Tenryū river. Meanwhile, two large granitic bodies are present on both sides of the " tail " part: the Inagawa granite in the western side and the complex of the Ichida granite and the Ōtagiri granite in the eastern side. The Inagawa granite, which is a syn-kinematic granite of the Ryōke plutonism builds the main part of the Kiso mountain range or the so-called Central Alps of Japan together with the Kisokoma granodiorite. The distribution of the Ōtagiri granites and the Ichida granite in the eastern side is complicated. It is inferred that the Ōtagiri granite intruded after the emplacement of the Ichida granite, because the weak flow structures of the former traverse obliquely those of the latter.

Small granodiorite body which intruded probably along the Komagane fault is recognized at the eastern wing of the dome, and is denominated as the Akagi granodiorite.

The direction of faults are characteristic; the Koyashiki fault and Ōtagiri fault show the NE-SW trend, the Komagane fault and Nakatagiri fault the N-S trend. They have common features in that they have wide sheared zones composed of small scale shear planes and yet have little throw except the Ōtagiri fault. The fault breccias which are metamorphosed to hornfelses are recognized along the Koyashiki fault. It is evident that the Koyashiki fault had been activated before the regional metamorphism were taken place.

The Ōtagiri fault is an estimated fault, but its exposures have not yet been confirmed in the field.

The outline of petrography

Biotite slate

The stratification and texture of the original rocks which consist of alternation of clayslates and sandstones intercalated with limestones and basic tuffs are preserved in the biotite slates. The alternation is folded and the sandstone layers are sometimes torn to pieces. Quartz, recrystallized biotite, sericite and graphite pigments are observed in thin sections.

Schistose hornfels I

The schistose hornfelses I are reddish brown in colour and have weak cleavages, though the structures of the original rocks are still preserved. The constituent minerals are completely recrystallized to quartz, biotite, muscovite, graphite and opaque minerals. Biotite and graphite exhibit a preferred orientation.

Schistose hornfels II

The structures of the original rocks are gradually obliterated and the well-marked foliations are developed in the schistose hornfelses II. The essential minerals are quartz, plagioclase, biotite and muscovite with mosaic texture. Andalusite, cordierite, garnet and tourmaline are sometimes present.

Banded gneiss

The banded gneisses are characterized by the foliations which are defined by the alternation of biotite-rich layers and quartzo-feldsparthic layers. Fibrous sillimanite, cordierite, garnet, tourmaline and opaques are recognized besides the main constituents such as quartz, plagioclase, muscovite and biotite.

Cordierite hornfels

Cordierite hornfelses are reddish brown or dark brown in colour, characterized by dark coloured pinitized cordierite spots 1–15 mm in diameter.

Ōtagiri granite

The grayish coloured variety of the Ōtagiri granites is fine-grained two mica granite. The granite which intruded in the centre of the dome is massive, while those intruded as sheets show weak foliations. The granites which intruded along the Ōtagiri fault represent rather cataclastic texture. The essential constituents are quartz, potash-feldspar, plagioclase, muscovite and biotite, and the accessary minerals are garnet, tourmaline, zircon, apatite, sericite and opaques. These mineral assemblages are the same as those of the leucoclatic aplitic variety.

Kisokoma granodiorite

The Kisokoma granodiorites are gray coloured and medium-grained rocks with very weak flow layers. The essential constituents are quartz, potash-feldspar, plagioclase, biotite and hornblende, and the accessary minerals are zircon, apatite, epidote, sphene and opaques.

Akagi granodiorite

The Akagi granodiorites are gray coloured and medium-grained rocks and are conspicuously weathered in the field. Their mineral assemblages are very similar to those of the Kisokoma granodiorites, though the Akagi granodiorites show a cataclastic texture.

The setting of subareas

From the standpoint of geological structure, the region is divided into the two districts by the Koyashiki fault. The northwestern district is occupied by the biotite slate and the schistose hornfels I, exhibiting a monotonous monoclinic structure, while the southeastern district is represented by the dome structure in question. It consists of three different units: the northwestern wing which lies between the Ōtagiri fault and the Koyashiki fault, the main district associated with the intrusion of the Ōtagiri granites and the " tail " district which stretches to the south. No structural boundary is recognized between the main district and the " tail " district of the dome. From the structural point of view, however, the main district is an oval shaped dome with its longer axis in the direction NNE-SSW, while the " tail " district exhibits a minoclinic structure inclined to the west. Although the foliations of the southeastern wings of the main district incline to the south-east, they gradually turn into and dip to the northwest near the southern part of the Ōtagiri river and change into a monoclinic structure.

From the evidence above mentioned, four subareas are discriminated from north to south as follows:

(I) The district to the north of the Koyashiki fault,
(II) The district between the Koyashiki fault and the Ōtagiri fault,
(III) The main district of the Ōtagiri dome,
(IV) The " tail " district of the Ōtagiri dome.

The megascopic structural analysis in each subarea is explained below.

Megascopic structure

A) Structural elements

i) Foliation

A kind of megascopic *s*-plane is widely developed in the metamorphic rocks. It will be referred to as foliation throughout the present paper. It is due to dominant isotropical arrangement of platy minerals such as biotite. In the banded gneisses, well-marked foliations are defined by the alternation of layers enriched in mica or quartzo-feldsparthic minerals. They gradually become obscure with decreasing metamorphic grade and sometimes obliterate in the zone of biotite slate, while in contrast stratifications become more distinct.

Very weak foliations are recognized in the Ōtagiri granites and comparatively obvious foliations, which are parallel or subparallel to that of country rocks at the contacts are noticed especially along the Ōtagiri fault as well as some sheet-like bodies.

Now, the relation between the foliation and the stratification in some localities offers an interesting problem. It is observed that the folded stratifications are traversed obliquely or almost perpendicularly by the well-marked foliations as shown

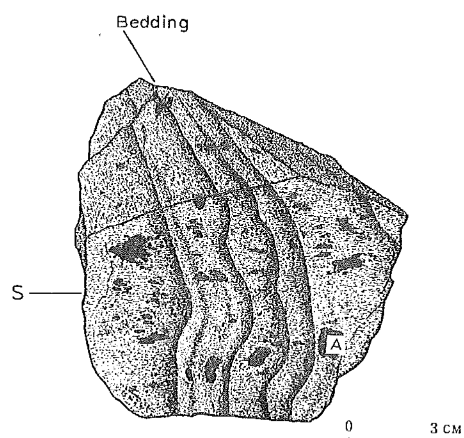

Fig. 1
Crossing of two planer structures; foliation (*S*) and bedding plane. (From the Inutagiri river).
A: Andalusite

in Figure 1. Most of these phenomena are observed along the midstream of the Inutagiri river which belongs to the subarea II and subarea III. This type of overlapping of deformations is common there. A quite similar deformation was found in the northernmost part of the region which belongs to the subarea I. Though the whole aspect of the deformation is not yet thoroughly clear, it can presumably be interpreted in two ways; the one is that the pre-Ryōke deformation took place entirely over the region, and the other is that the deformation took place mainly in the outer zone at the initial phase of the regional metamorphism. However, the trends of the folding axes of the stratifications in question are subparallel to the regional trend of the major folding axes of the non-metamorphosed or slightly metamorphosed Paleozoic formation in the regions further to the north and the northwest of the present district (cf. KATADA, et al., 1961). So the present author concludes that a regional folding of the Paleozoic strata took place throughout the subareas prior to the mineralization of biotite blades, i.e., the formation of the foliation.

Somewhat similar phenomena were observed in the subareas III and IV, as shown in Figure 2. Some parallel arrangements of biotite blades traverse the close-

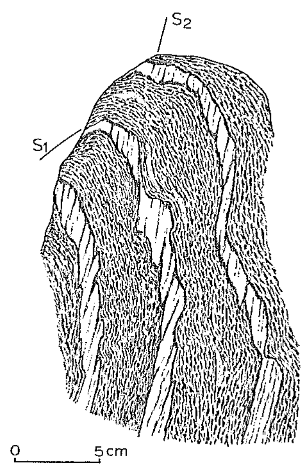

Fig. 2
Crossing of two planer structures in banded gneiss; foliation S_1 and S_2. S_2 is observed only in the folded quartzofeldsparthic band and is estimated to be caused by a kind of shear fold. (From the Ōtagiri river)

folded quartzo-feldsparthic bands of the banded gneiss at their crest. It is likely that the deformation occurred prior to the mineralization of biotite. This is a kind of shear folding, which is naturally different from the case above mentioned. These problems will be discussed in another paper.

Notwithstanding these instances, it is asserted that the foliations are evidently parallel to the stratification for the most part of the region.

ii) Lineation

The most dominant lineation in the high grade metamorphic rocks in the region is a short wave-length unduration on the foliated plane, or the so-called " microfold ", and linear arrangements of mineral grains such as biotite are also marked. They are parallel to the axes of the microfold. In the low grade metamorphic rocks, the linear arrangement of mineral grains defines the lineation in common, but it is very weak or undetectable in the biotite slates. These are referred to L_{m-2}.

Other lineations which have rather different trend from the lineation L_{m-2} are clarified by statistical analysis in the subarea III. Their appearance is quite similar to that of L_{m-2}, and both are not found together in the same specimen. Being considered as a deformation formed by the intrusion of the Ōtagiri granites, they are distinguished from L_{m-2} and referred to L_{m-3}.

Some noticable specimens from the midstream of the Nakatagiri river in the subarea IV, as shown in Figure 3, have distinct fine crinkles obliquely crossing the unduration (L_{m-2}). They are defined to L_{m-1}.

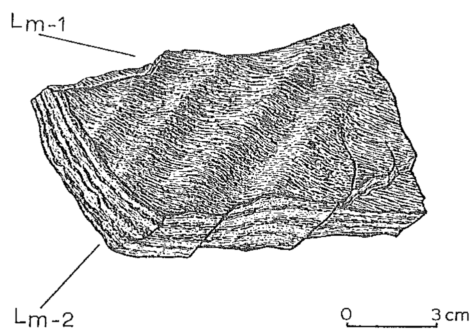

Fig. 3
Crossing of two lineations L_{m-1} and L_{m-2}.
(From the Inutagiri river)

In the Ōtagiri granites the lineation is generally unobservable in the hand specimen. Microscopically, however, it can be deduced from the fabrics of preferred orientation of biotite blades. Generally, two lineations are revealed from each fabric (Figs. 14-j, 14-k and 14-1); the one is clear and denominated as L_{g-2}, and the other is rather indistinct and denominated as L_{g-1}.

iii) *B*-axes

For megascopic and microscopic petrofabric analysis it is very important to decide whether a lineation is parallel or normal to the direction of movement. Actually there has been much discussion on this problem.

In the high grade metamorphic rocks a kind of shear fold as shown in Figure

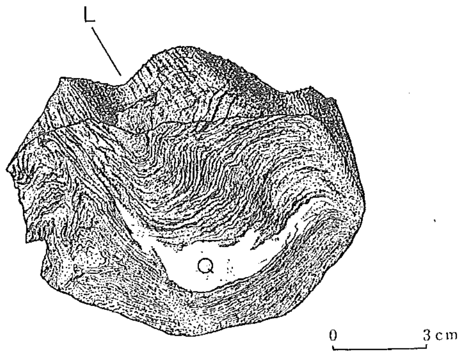

Fig. 4
Sketch showing the relation between shear fold and lineation (L).
The axis of shear fold is parallel to the lineation.
Q: quartz pool.
(From the Ōtagiri river)

4, is sometimes recognized, and the folding axes obviously coincide with lineation L_{m-2} or L_{m-3}. Moreover, even in the subarea I, for example, in which metamorphic rocks preserve monoclinic structure with their major folding axes to the northeast, lineations L_{m-2} are parallel to the major folding axes. The most conclusive for the matter is the relation between maximum of lineation diagram and estimated position of high concentration of β-diagram in each subarea. The letters " β " in Figures 5, 7, 9 and 11 represent the position of high concentration of β-diagrams in each subarea. Superposing β-diagrams upon the homologous lineation diagrams, each " β " corresponds exactly to each maximum of lineation diagram. These facts afford sufficient proofs that lineations L_{m-2}, and L_{m-3} are normal to the direction of the movement, namely, *b*-lineation and these metamorphic rocks are *b*-tectonites.

There is no evidence to decide whether lineation L_{m-1} is *a*-lineation or *b*-lineation, but it is assumed to be residual lineations normal to the direction of preceding movement, which took place before the deformation corresponding to L_{m-2}. Therefore, the lineation L_{m-1} is also a *b*-lineation.

The lineations L_{g-1} and L_{g-2} of the Ōtagiri granites estimated from the preferred orientation of the biotite crystals are considered *b*-lineation because of the following facts;

i) Generally two or more prominent shear planes being interpreted to be caused by flattening are recognized in the biotite fabrics, and the lineations L_{g-1} and L_{g-2} represent the intersections of these shear planes.

ii) The specimens are collected from the larger masses and a sheet which intruded parallel or subparallel to the country rocks, and the azimuth and the plunge of the lineations are almost E-W and horizontal. If they are *a*-lineation, therefore, the direction of the intrusion of the Ōtagiri granites could not be explained.

B) Description of the subareas

i) Subarea I

Since the northwestern margin of the subarea corresponds to the biotite slate zone which is slightly metamorphosed, the foliations are often indistinct, while the stratification is distinct throughout the whole subarea. The informations obtained from the field observations clarify that the foliation superposes in parallel to the stratification, and consequently the stratification together with the foliation is defined as *s*-surface.

As shown in Figure 5, the maximum of π-diagram for *s*-surface is situated in the second quadrant and has the azimuth and plunge of ca. N 45°W, 75°NW. Accompanying submaxima, the maximum area shows a tendency to extend on a great circle to the centre. The diagram represents the monoclinic structure of the subarea with its trend of N 45°E dipping to the southeast.

In the fabric diagram for lineation L_{m-2} (Fig. 6), the maxima are situated on the periphery in the first and the third quadrants, taking antipodal positions. The maximum in the third quadrant is more prominent than that in the first and then it signifies that the lineation L_{m-2} in the subarea shows its trend with N 45°E and dips slightly to the southwest.

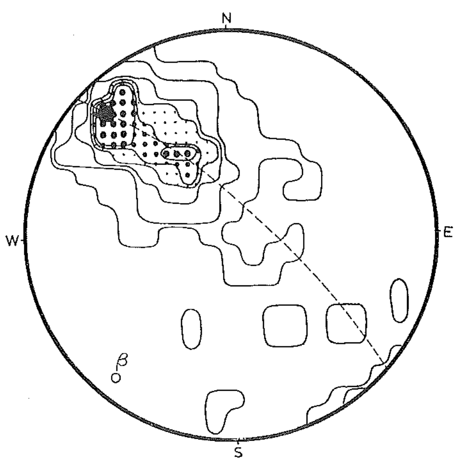

Fig. 5
π-diagram for *s*-surface in subarea I. (154 *s*-surfaces) Contours 14–12–10–8–6–3–0.6%

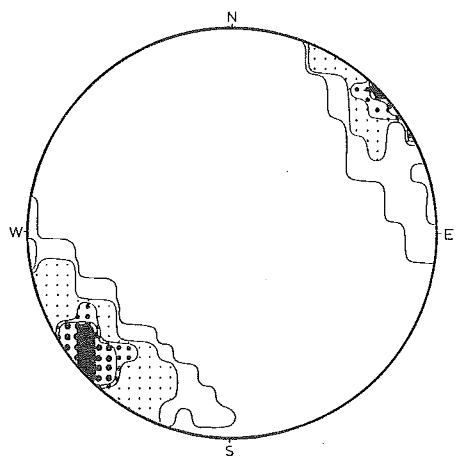

Fig. 6
Lineation (L_{m-2}) diagram in subarea I. (97 lineations) Contours 12–9–6–3–1%

ii) Subarea II

The maximum of the π-diagram for s-surface (Fig. 7) is in the forth quadrant, and its azimuth and plunge are about N 35°W and 60°–70°SW. The submaxima extend along the great circle to the centre showing as if it holds monoclinic structure. Though the subarea includes a part of the Ōtagiri dome as plainly shown in Plate 8, such structure is not manifested in the diagram because of scarcity of data. Only 30 lineations L_{m-2} obtained from the subarea are projected directly with dotts in Figure 8. They show an indistinct maximum in the first quadrant, with a trend and plunge of approximately N 20° E and 75° NE.

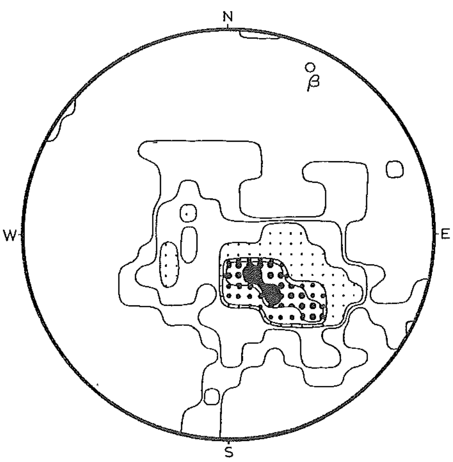

Fig. 7
π-diagram for s-surface in subarea II. (99 s-surfaces) Contours 15–10–7–4–2–1%

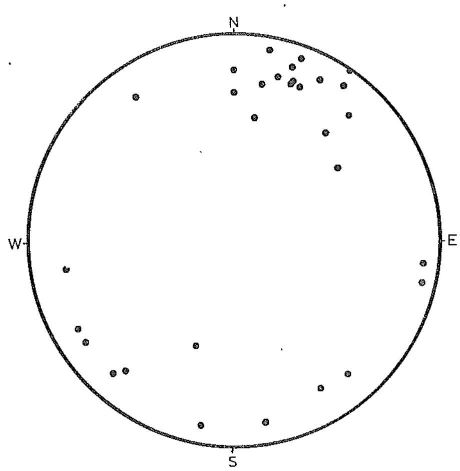

Fig. 8
Lineation (L_{m-2}) diagram in subarea II. (30 lineations)

iii) Subarea III

The π-diagram for s-surface and the fabric diagram for lineations of the subarea III are shown in Figures 9 and 10.

The maximum of the π-diagram for s-surface are situated in the third and fourth quadrants. In the third quardrant one maximum exists with its azimuth and plunge of about N 55° E and 50° SW, and in the fourth quardrant two maxima are recognized; the prominent one with an azimuth and plunge of about N 70° W and 45° SE, and the other with an azimuth and plunge of N 25° W and 45° S. Since the eastern wing of the dome is overlain by the Tenryū gravel, no maxima are recognized in the first and second quadrants. Taking the submaxima in account, the π-diagram shows a tendency to take a half small circle, which represents the dome structure.

The fabric diagram for lineations is characteristic; the lineations in the northern half of the subarea concentrate into the first quadrant and those in the southern half are in the third quardrant. In the first quadrant two maxima are recognized; the lineation L_{m-2} and the lineation L_{m-3}. The azimuth and plunge of the former are about N 50° E, 15° NE, and those of the latter are about N 30° E, 30°N, and both have antipodal submaximum in the third quadrant. They are two pairs of arched lineations which intersect each other, and their angle distance is about 30°.

The lineations L_{g-1} and L_{g-2} which are the *b*-lineations are plotted in the lineation diagram in question with black dotts (L_{g-2}) and white circles (L_{g-1}).

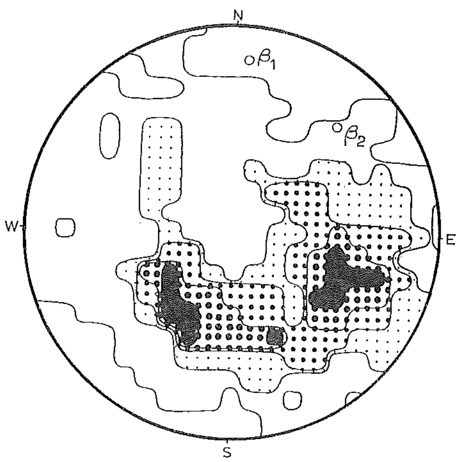

Fig. 9
π-diagram for *s*-surface in subarea III. (388 *s*-surfaces) Contours 5-4-3-2-1%

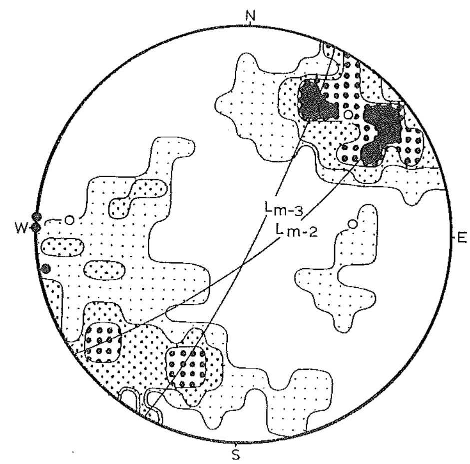

Fig. 10
Lineation (L_{m-2} and L_{m-3}) diagram in subarea III. (102 lineations) Contours 7-5-3-1%
The white circles represent the lineation L_{g-1} and the black dotts represent the lineation L_{g-2}

iv) Subarea IV

The *π*-diagram for *s*-surface and the fabric diagram for lineation L_{m-2} of the subarea IV are shown in Figures 11 and 12.

In the *π*-diagram for *s*-surface, maximum is preserved in the fourth quadrant with its trend and plunge of about N 25° W and 25° SE. Reflecting the fact that the subarea IV includes both dome structure and monoclinic structure, some concentration in the second quadrant is recognized, and consequently the trend of the foliation changes from NNE-SSW to N-S and, the maximum area as well as submaximum area exhibits a tendency to stretch on the great circle to the first quadrant in the diagram.

The maximum in the fabric diagram for the lineation L_{m-2} is situated in the third quadrant, having its azimuth and plunge of about N 60° E and 50° SW. It shows that the trends of the lineations L_{m-2} are steeper in comparison with those in the subarea III.

The overcrossing fine clinkles (L_{m-1}) are projected on the lineation diagram with dotts.

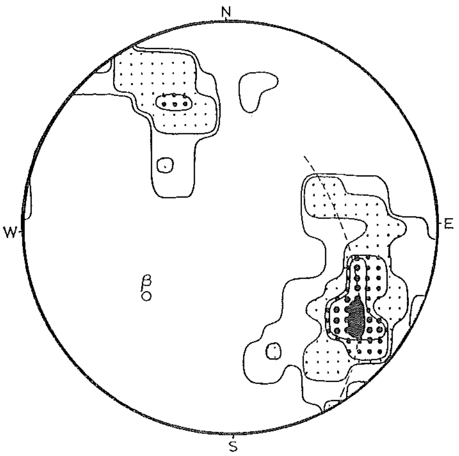

Fig. 11
π-diagram for *s*-surface in subarea IV. (65 *s*-surfaces) Contours 11–9–6–3–1%

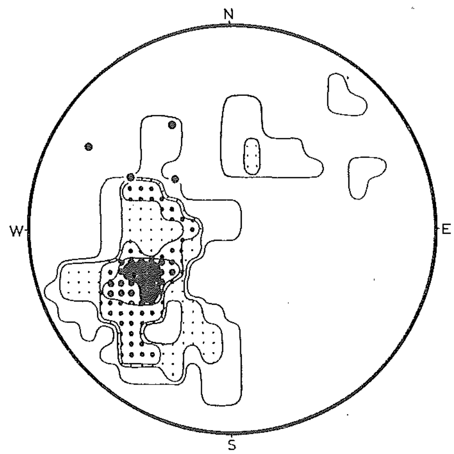

Fig. 12
Lineation (L_{m-2}) diagram in subarea IV. (50 lineations) Contours 12–8–6–4–2%
The black dotts represent the lineation L_{m-1}

C) Discussion

From the patterns of the fabric diagrams for *s*-surface, the difference of the geological structure between the subarea I and the other subareas is shown clearly, so that the structural significance of the Koyashiki fault in this region is also evident, dividing the region into the doming area and the non-doming area. Thus the subarea I holds a monoclinic structure with azimuth and plunge of N 30° W and 35°–80° SE, while the subareas II, III and IV are involved in the Ōtagiri dome. Hitherto it has been referred that only the southeastern areas of the Ōtagiri fault represent a dome structure and the northwestern area which lies between the Ōtagiri fault and the Koyashiki fault (namely, subarea II) preserves a monoclinic structure (KATADA, et al., 1961). And they have concluded that the Ōtagiri fault represented a structural boundary between the " central " zone and the " outer " zone of the region when the dome was accomplished. They stressed the structural significance of the fault and designated it the " Ōtagiri-Kisokoma-Line ".

It is, however, clarified by the present author that the northwestern district which is restricted to the northwest of the Koyashiki fault (subarea II) also holds the northern and western wings of the Ōtagiri dome. The subarea III occupies the main part of the Ōtagiri dome and exhibits an oval shape dome structure having the trend of its long axis to NNE. The subarea IV shows a monoclinic structure dipping to the west and represents the " tail " part of the Ōtagiri dome.

As the foliations of the subareas dipping to the west surround the granitic complex of the Ichida granite and the Ōtagiri granite, it may be possible to describe that the " tail " part presents the western half of the other dome structure in which the Ōtagiri granite and the Ichida granite in the centre.

Two characters will be pointed out as to the lineations of the doming area as follows.

i) The lineation L_{m-2} represents an arched structure as a whole of the doming area having its appex in the subarea III.

ii) The lineation L_{m-3} different in orientation from the lineation L_{m-2}, is recognized only in the subarea III, and it is closely correlated to the lineation L_{g-2} which is a *b*-lineation of the Ōtagiri granites.

The first characteristic feature clearly shown in Plate 8, is especially distinct, when the lineation diagram in the subarea III is compared with that in the subarea IV. The lineations L_{m-2} become to plunge steeper to the south, and they plunge to the north in the northern half of the subarea III, as described before. While they plunge to the north in the subarea II though their original trend may be modified somewhat by the Ōtagiri fault. These facts seem to support that the lineation L_{m-2} is originated by the up-doming of the Ōtagiri dome preserving its centre in the subarea III.

As to the second characteristic point, two conspicuous pairs of the lineations are found in the fabric diagram for the lineation only in the subarea III (Fig. 10). They are considered as arched feature of the two different systems of the lineations. Their trends are N 50° E and N 30° E respectively, of which the former is the lineation L_{m-2} and the latter is the lineation L_{m-3}. The inference that the lineation with the trend of N 50° E is original (L_{m-2}), will be supported by following facts.

i) The direction of the lineation with the trend of N 50° E in the subarea III is parallel to the lineation L_{m-2} in the subarea IV. If the lineation with the tend of N 30° E is the lineation L_{m-2}, the direction of tectonic transport of the doming area can not be explained reasonably.

ii) The Ōtagiri granites intrude only in the subarea III. Lineations L_{g-2} are defined as a *b*-lineation from biotite fabrics. They are concentrated to the periphery near the west of the diagram (Fig. 10), so that an *a*-lineation of the Otagiri granites, if ever exists, will probably be situated on the N-S axis of the diagram. Therefore, the lineation with the trend of N 30° E approximately assumes a trend bisecting the angle between the lineation with N 50° E trend (L_{m-2}) and a supposed *a*-lineation of the Ōtagiri granites. The lineation with a trend of N 30° E is assumed to be reoriented from the lineation with the trend of N 50° E by the intrusion of the Ōtagiri granites.

Microfabrics

The statistical analysis of mineral orientations is carried out on twelve specimens including schistose hornfelses, banded gneisses and the Ōtagiri granites. The orientations of quartz, biotite and muscovite are measured, and their fabric diagrams are prepared from the thin section orientated parallel or subparallel to the *ac*-plane, except in the case of the specimen 1 (Figs. 13-a, 14-a and 15-a) which is orientated parallel to the *bc*-plane.

The mineral assemblages are rather simple. In the metamorphic rocks, quartz and biotite are predominating, and other important minerals are muscovite and plagioclase, while sillimanites are recognized especially in banded gneisses. Interstitial quartz, plagioclase, potash-feldspar, biotite and muscovite are common in the Ōtagiri granites.

A) Quartz

Quartz grains generally show xenomorphic equigranular occurrence in the metamorphic rocks, but large porphyroblastic quartz with unduratory extinction is often found in banded gneisses. Large interstitial quartz grains are common in the Ōtagiri granites, and small granular grains included in other minerals are also found. The unduratory extinction and fractured splinters parallel to optic axes are common among them. Similar phenomena are also recognized in the interstitial grains, large porphyroblastic crystals and quartz grains in veinlet in the high grade metamorphic rocks, but their unduration is comparatively weak.

Roughly speaking, the orientation of quartz axes [0001] of the metamorphic rocks and of the Ōtagiri granites shows a tendency to hold the peripheral girdles or the cleft girdles in respect to the fabric axis B as a rule. These fabrics are classified into four types from the standpoint of symmetry and girdle pattern.

The first type is the quartz fabrics of the specimens 2, 3, 4, 6, 7, 8 and 10 (Figs. 13-b, 13-c, 13-d, 13-f, 13-g, 13-h and 13-j). The specimens 2 and 3 are collected from the subarea II; 4, 6 and 10 from the subarea III; 7 and 8 from the subarea IV. Their fabrics are characterized by the complete *ac*-girdle with maxima and submaxima without regard to the subareas and rock species. Having maxima and submaxima on a small circle, the pattern of each fabric has a tendency to assume a complete cleft girdle, of which the centre coincides with the fabric aixs B, namely *b*-lineation. It is clear that the symmetry of each fabric is approximately monoclinic with a single symmetry plane normal to L_{m-2}, L_{m-3} or L_{g-2}.

The second type is the fabrics of the specimens 5 and 9 (Figs. 13-e and 13-i), of which the former is collected from the subarea III and the latter from the subarea IV. They exhibit characteristically double *ac*-girdles; the inner small girlde is incomplete and its symmetry is also indistinct. FAIRBAIRN and CHAYES regard that such a girdle is formed by residual orientation (FAIRBAIRN, H. W. and F. CHAYES, 1949). In the fabric of specimen 5, the outer girdle indicates compratively a clear cleft girdle with the girdle axis corresponding to the fabric axis *B*, while in

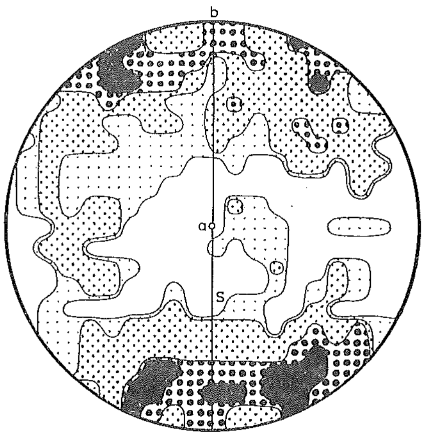

Fig. 13-a
Specimen 1, 300 quartz [0001] axes from schistose hornfels
Contours 4–3–2–1%

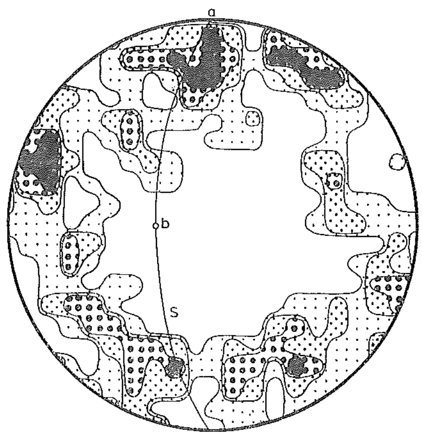

Fig. 13-b
Specimen 2, 300 quartz [0001] axes from schistose hornfels
Contours 2.5–2–1.5–1%

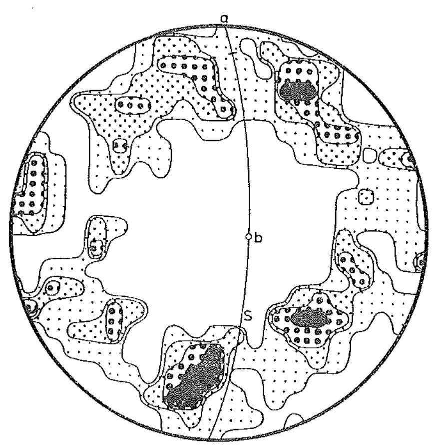

Fig. 13-c
Specimen 3, 300 quartz [0001] axes from schistose hornfels
Contours 3–2–1.5–1%

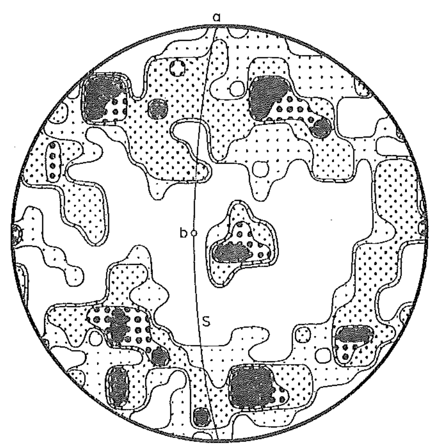

Fig. 13-d
Specimen 4, 300 quartz [0001] axes from banded gneiss
Contours 2.5–2–1.5–1%

the fabic of specimen 9 its pattern does not form any girdle, though a weak tendency to show the *ac*-girdle still remains. The symmetry of the fabric of specimen 5 is approximately monoclinic and that of specimen 9 is rather triclinic.

The third type is the fabrics of the specimens 11 and 12 (Figs. 13-k and 13-l), which are obtained from the Ōtagiri granite. The fabric pattern does not hold

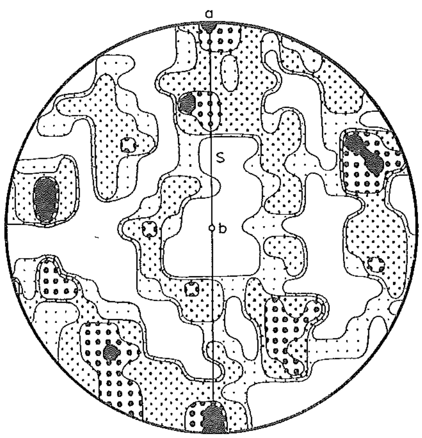

Fig. 13-e
Specimen 5, 300 quartz [0001] axes from banded gneiss
Contours 2.5–2–1.5–1%

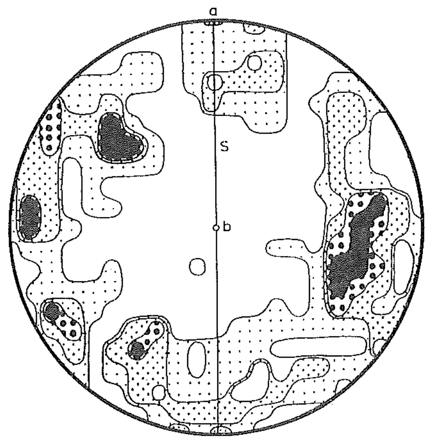

Fig. 13-f
Specimen 6, 300 quartz [0001] axes from banded gneiss
Contours 3–2.5–1.5–1%

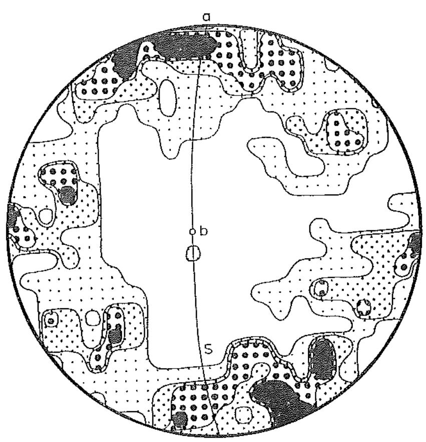

Fig. 13-g
Specimen 7, 307 quartz [0001] axes from banded gneiss
Contours 2.5–2–1.5–1%

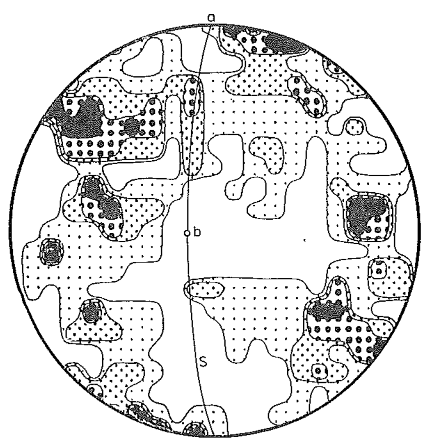

Fig. 13-h
Specimen 8, 304 quartz [0001] axes from banded gneiss
Contours 2.5–2–1.5–1%

any girdle and it may be sure that the symmetry of the fabrics is approximately triclinic. Although the fabric pattern seems to be correlated with L_{g-2}, it is recognized that there is no correlation between the fabric pattern and L_{g-1}.

The fourth type is the fabric of the specimen 1 (Fig. 13-a), collected from the northern boundary of the Ōtagiri granite which intruded along the Ōtagiri fault.

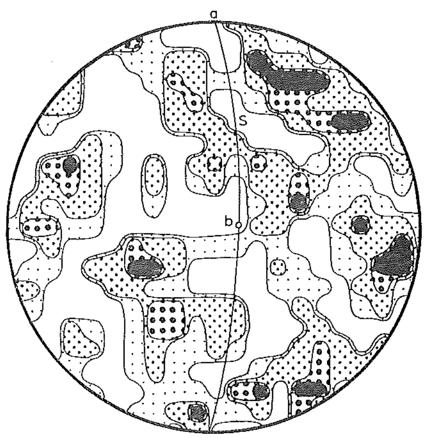

Fig. 13-i
Specimen 9, 300 quartz [0001] axes from banded gneiss
Contours 2.5–2–1.5–1%

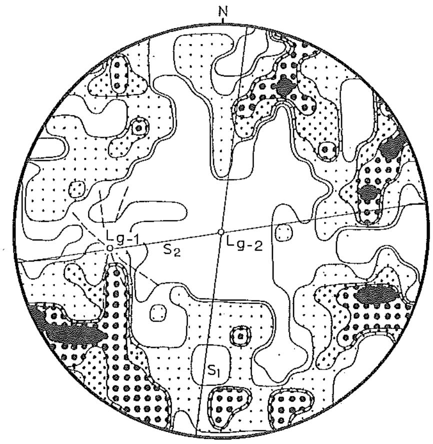

Fig. 13-j
Specimen 10, 292 quartz [0001] axes from the Ōtagiri granite
Contours 3–2.5–2–1.5–1%

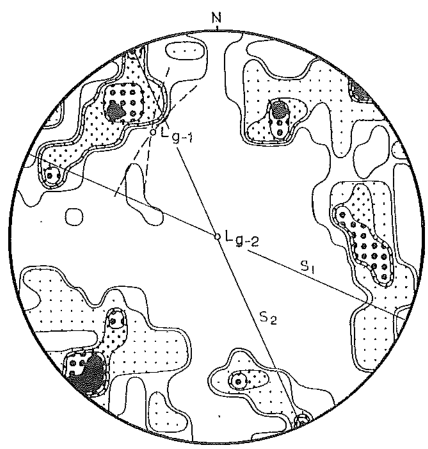

Fig. 13-k
Specimen 11, 144 quartz [0001] axes from the Ōtagiri granite
Contours 6–4–3–2–1%

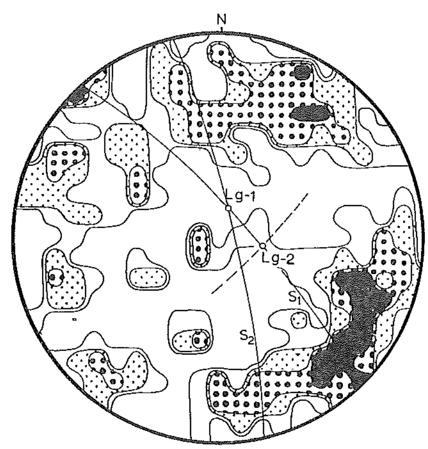

Fig. 13-l
Specimen 12, 198 quartz [0001] axes from the Ōtagiri granite
Contours 3–2–1.5–1%

It is characteristic that very distinct foliation and lineation are marked by the parallel alignments of a lot of tourmaline, biotite and muscovite blades. Even if the fabric data are rotated for 90 degrees about the fabric axis *C* it is evident that not girdle will be presented, because its section is prepared parallel to the *bc*-plan of the fabric. The symmetry of the fabric is approximately monoclinic with a symmetry plane parallel to the *ac*-plane of the fabric. The fabric pattern of the specimen differs entirely from others.

Discussion

The quartz fabrics can be classified into four types from the viewpoints of the symmetry and girdle pattern as stated above, although intermediate types are common.

Of these the first type is the most predominant normal type of quartz fabric in the region, except specimens 10, 11 and 12 which are the fabrics of the Ōtagiri granites.

It is characteristic to the first type that it shows a distinct *ac*-cleft girdle of which centre coincides with the fabric axis *B*, and the maxima and submaxima exhibit approximately monoclinic symmetry. This suggests that the quartz fabric can be correlated closely with the lineation L_{m-2} or L_{m-3} and foliation *S*. Therefore, it is meaningless to discuss the *ac*-girdle and maxima separately.

Many hypotheses have been proposed on the mechanisms of the preferred orientation of quartz fabrics, but no conclusive theory which explains both girdle and symmetry at the same time has not yet been obtained.

According to FAIRBAIRN and CHAYES (1949), one of hypotheses appropriate for the interpretation of quartz girdle and symmetry is the fracture hypothesis, firstly proposed by SANDER (1930) and later developed by GRIGGS and BELL (1938). It is based on the assumption of rotational movement of fractured splinters of quartz grains about *b*, probably along a shearing plane.

Recently, however, TURNER and WEISS (1963) have rejected this hypothesis on the evidence that no proof of actual slip plane associated with the rotation is observed in tectonites, and that the patterns explained by the fracture hypothesis are well developed in the high grade metamorphic rocks which have been influenced far more by recrystallization than by deformation. They lay much stress on the effect of the recrystallization under the penetrative stress and explain speculatively the fabric pattern as the superposed subfabrics which hold an orthorhombic symmetry in most cases.

From their studies on the *ac*-girdle of quartz fabrics in the migmatite domes of the southern Hidaka metamorphic belt, however, KIZAKI (1956) and KASUGAI (1957) have assumed an existence of actual slip planes from the evidence that the distribution of axes within individual quartz grains exhibiting undulatory extinction is surrounding about *b*. Quite similar evidences are also found in the fabrics of the

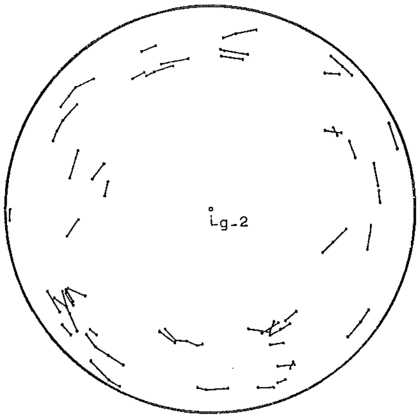

Fig. 13-m
Trend lines of axes within individual strained quartz grains (undulatory extinction) from the Ōtagiri granite

present region especially in the high grade metamorphic rocks and the Ōtagiri granites (Fig. 13-m). Since the fractured splinters parallel to quartz axis [0001] are found by the microscopical observation in the present case, suggesting the internal rotation of quartz grains about *b*, the fracture hypothesis seems to explain them much better than TURNER and WEISS's hypothesis. The distribution of quartz axes resulting in the *ac*-girdle may represent the loci of axes of the grains which either have not yet attained desirable positions or have been shifted out of such desirable positions by subsequent rotation. Probably the maxima and submaxima represent the approximate desirable positions. The fabric pattern of the first type is recognized in the metamorphic rocks regardless to the subareas or metamorphic grades. The movement which caused rotational movement is regarded as the partial movement, correlated closely with the up-doming of the Ōtagiri dome.

The second type is characterized by double girdles, which are considered by FAIRBAIRN and CHAYES (1949) as residual orientation. The field occurrence of the specimens 5 and 9 is well in conformity with the interpretation. In the specimen 5, collected from a contact of the gneiss with the sheet of the Ōtagiri granites at about the centre of the dome, some influence of the intrusion of the Ōtagiri granite is expected. Fine clinkles (L_{m-1}) are overcrossed obliquely by microfolds (L_{m-2}) in specimen 9, and some residual fabrics in the orientation of quartz axes are also expected.

Moreover, the fourth type is considered to be influenced remarkably by the successive intrusion of the Ōtagiri granites after the Ōtagiri fault took place, so that the original fabric has been modified conspicuously.

The fabrics of the Ōtagiri granites are classified as the first type (Fig. 13-j) and the third type (Figs. 13-k and 13–l). In comparison with the patterns of the both types of the metamorphic rocks, it can be concluded clearly that the Ōtagiri granites were deformed differently from the deformation of the metamorphic rocks. However, the existence of the fabric of specimen 10 (Fig. 13-j) proves that there are also some similar modes of deformation of the granites with those of the metamorphic rocks. From the field evidences as well as the results of other petrofabric studies, it seems likely that the Ōtagiri granites intruded subsequently into the metamorphic rocks which were doming up, and the features of the fabrics of the Ōtagiri granites reflect such affairs.

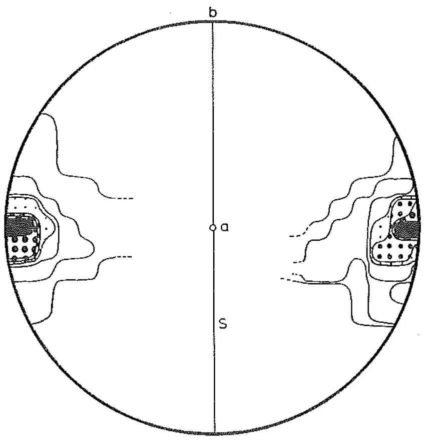

Fig. 14-a
Specimen 1, 150 cleavage poles of biotite from schistose hornfels
Contours 22–18–14–10–6–2–0.6%

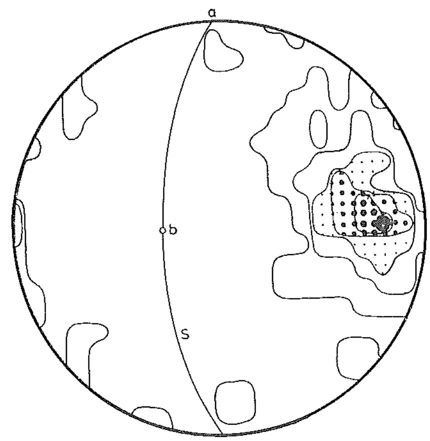

Fig. 14-b
Specimen 2, 100 cleavage poles of biotite from schistose hornfels
Contours 20–15–10–6–3–1%

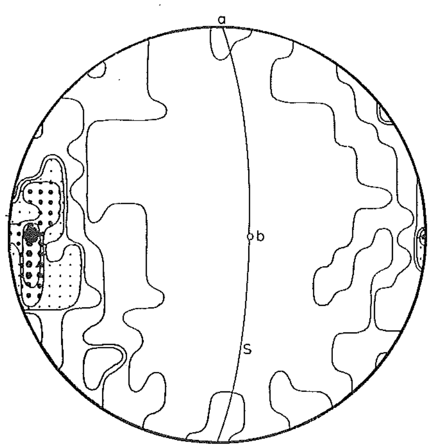

Fig. 14-c
Specimen 3, 150 cleavage poles of biotite from schistose hornfels
Contours 12–10–8–6–4–2–0.6%

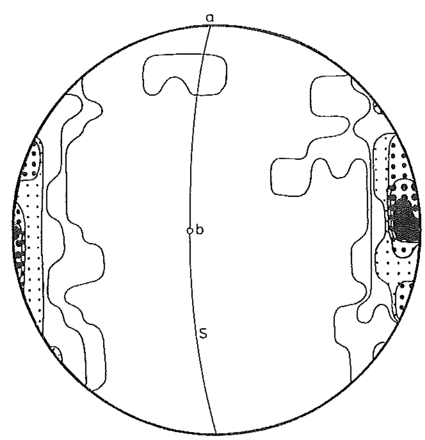

Fig. 14-d
Specimen 4, 150 cleavage poles of biotite from banded gneiss
Contours 14–12–8–4–2–0.6%

The quartz fabrics of the Ōtagiri granites are not related to the lineation L_{g-1}, in spite of their good correlation with the lineation L_{g-2}. KVALE (1953) described that the quartz grains reflect the deformation of a later stage than do micas. This was also supported by CRAMPTON (1958). Accordingly it seems likely that the lineation L_{g-1} is a relic which suggests a deformation of an earlier stage than that of the lineation L_{g-2}.

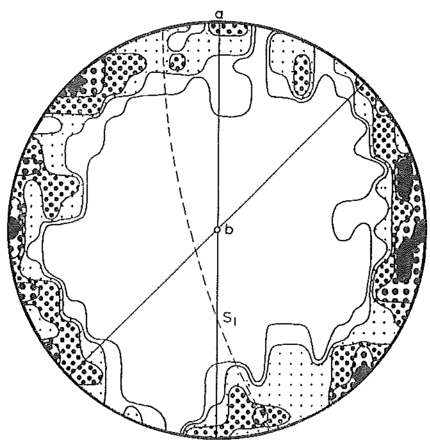

Fig. 14-e
Specimen 5, 109 cleavage poles of biotite from banded gneiss
Contours 7–5–3–2–1%

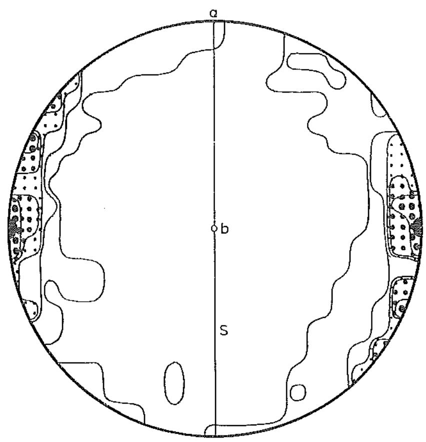

Fig. 14-f
Specimen 6, 158 cleavage poles of biotite from banded gneiss
Contours 14–10–8–6–2.5–0.6%

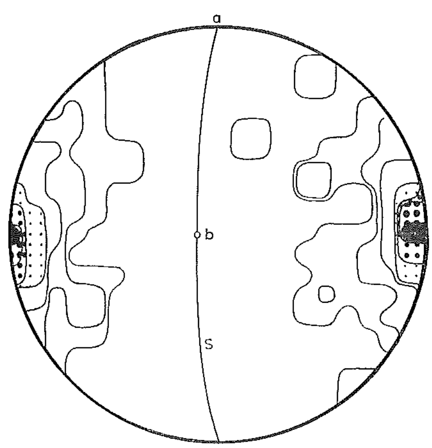

Fig. 14-g
Specimen 7, 157 cleavage poles of biotite from banded gneiss
Contours 18–16–12–8–4–2–0.6%

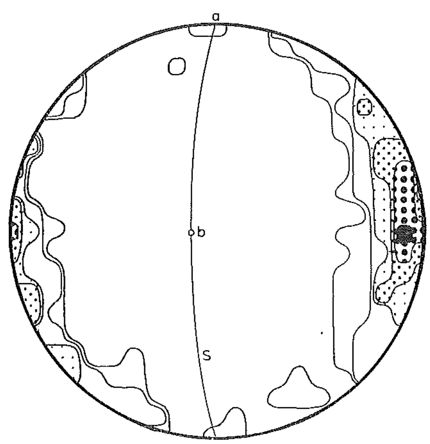

Fig. 14-h
Specimen 8, 164 cleavage poles of biotite from banded gneiss
Contours 12–10–6–4–2–1%

B) Biotite and Muscovite

Biotite blades are well aligned along foliation in the metamorphic rocks, and well-marked foliation defined by biotite-rich layers is distinct especially in the banded gneisses. With the progress of metamorphism, biotite blades increase in size and the postcrystalline deformation such as fracture, undulatory extinction and

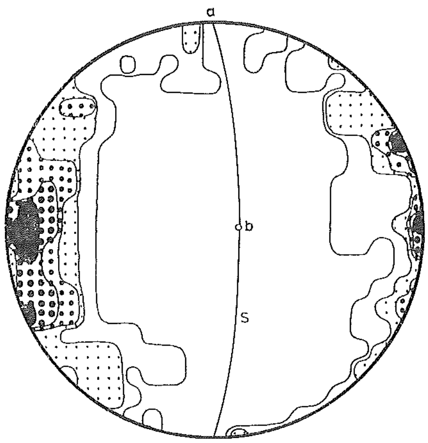

Fig. 14-i
Specimen 9, 152 cleavage poles of biotite from banded gneiss
Contours 10–6–4–2–0.5%

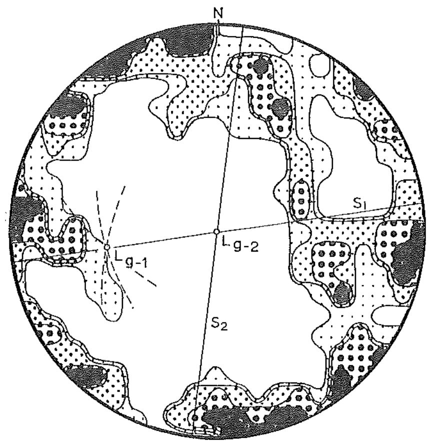

Fig. 14-j
Specimen 10, 150 cleavage poles of biotite from the Ōtagiri granite
Contours 3–2.5–2–1%

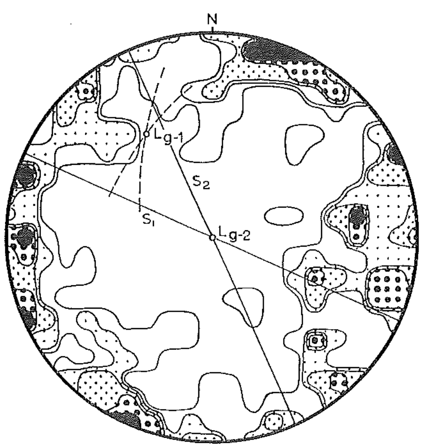

Fig. 14-k
Specimen 11, 100 cleavage poles of biotite from the Ōtagiri granite
Contours 5–4–3–2–1%

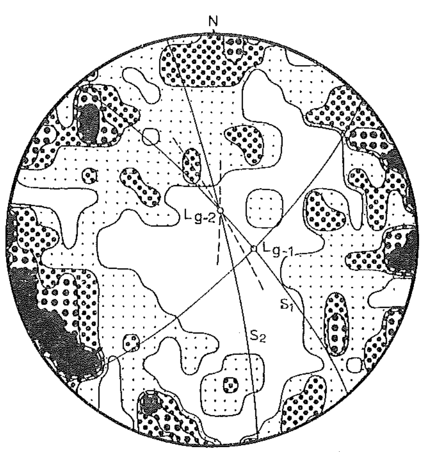

Fig. 14-l
Specimen 12, 105 cleavage poles of biotite from the Ōtagiri granite
Contours 4–3–2–1%

bending of biotites also become conspicuous. While muscovite blades are not so well-aligned as biotite, and sometimes large poikiloblastic blades are observed.

In the Ōtagiri granites, biotites are larger in size than those in the metamorphic rocks and their parallel alignment is obscure. Fracture and bending of biotites

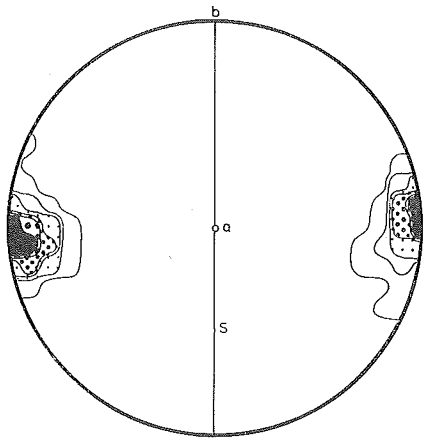

Fig. 15-a
Specimen 1, 100 cleavage poles of muscovite from schistose hornfels
Contours 25–20–15–10–5–1%

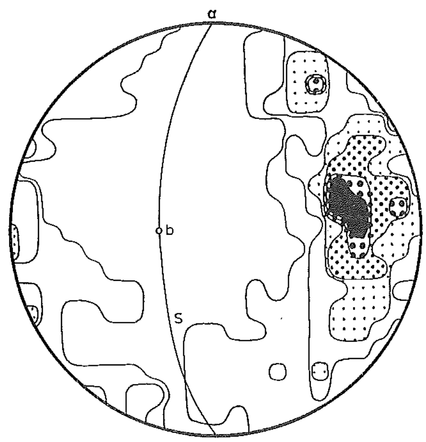

Fig. 15-b
Specimen 2, 167 cleavage poles of muscovite from schistose hornfels
Contours 7–6–4.5–3–2–1.5%

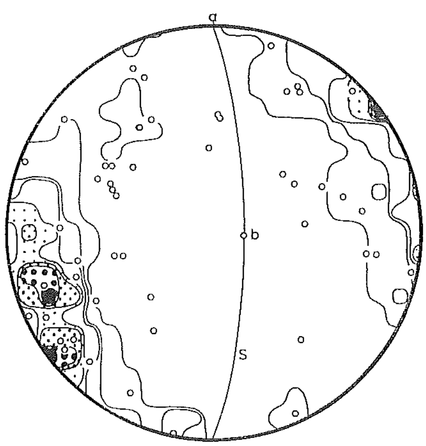

Fig. 15-c
Specimen 3, 161 cleavage poles of muscovite from schistose hornfels
Contours 11–10–8–6–4–2–1.5%
Open circles show the orientations of cleavage poles of muscovite in poikilitic nature

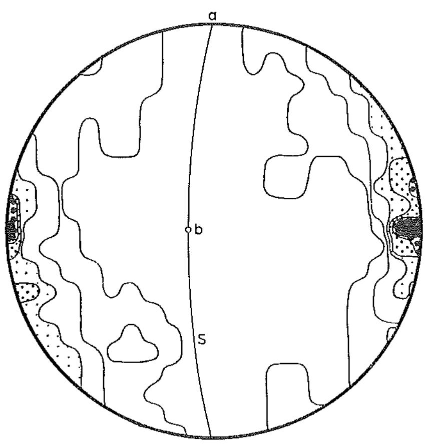

Fig. 15-d
Specimen 4, 155 cleavage poles of muscovite from banded gneiss
Contours 12–10–8–5–2.5–0.5%

are sometimes observed. Two kinds of muscovite blades are distinguished; the one is porphyroblastic or poikilitic crystals and the other is very fine grains of muscovite occurring along the cleavage planes of plagioclases.

The poles of cleavage planes of the biotite and muscovite blades are projected.

i) The biotite fabrics can be classified into following three types from the viewpoint of symmetry. The first and second types are the fabrics of the meta-

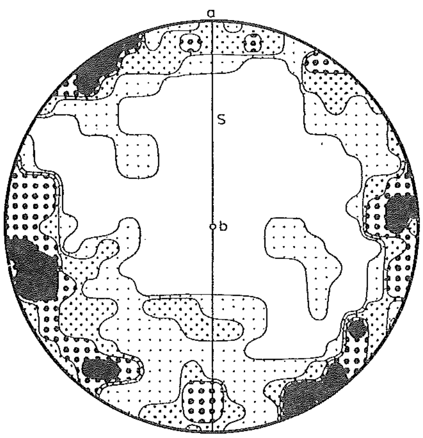

Fig. 15-e
Specimen 5, 103 cleavage poles of muscovite from banded gneiss
Contours 4–3–2–1%

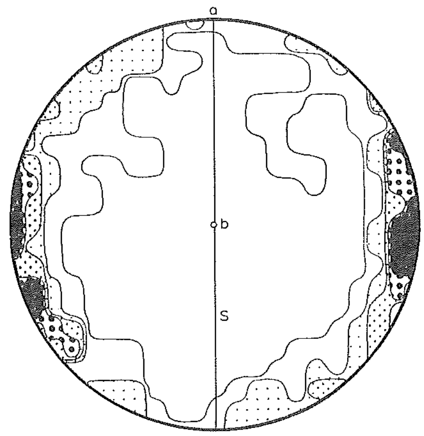

Fig. 15-f
Specimen 6, 150 cleavage poles of muscovite from banded gneiss
Contours 6–5–4–2–1%

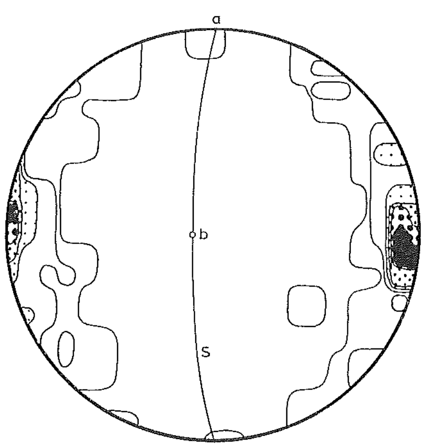

Fig. 15-g
Specimen 7, 100 cleavage [poles of muscovite from banded gneiss
Contours 15–12–9–6–3–1%.

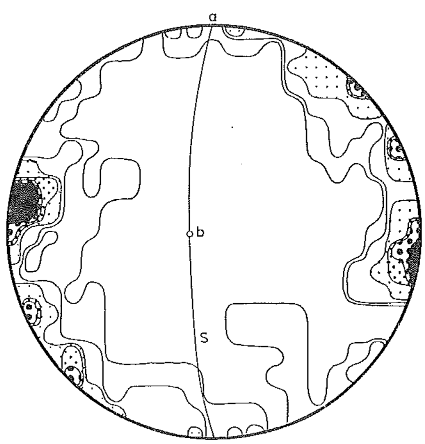

Fig. 15-h
Specimen 8, 100 cleavage poles of muscovite from banded gneiss
Contours 10–8–6–4–2–1%.

morphic rocks and the third type is those of the Ōtagiri granites.

The first type is the fabrics of specimens 1, 2, 4 and 7 (Figs. 14-a, 14-b, 14-d and 14-g). It is characterized by the fabrics with aproximately monoclinic symmetry. Each has a maximum at the fabric axis *C* showing weak development of incomplete *ac*-girdle, and defines strictly *s*-surface. The second type is the fabrics of specimens 3, 5, 6, 8 and 9 (Figs. 14-c, 14-e, 14-f, 14-h and 14-i) which

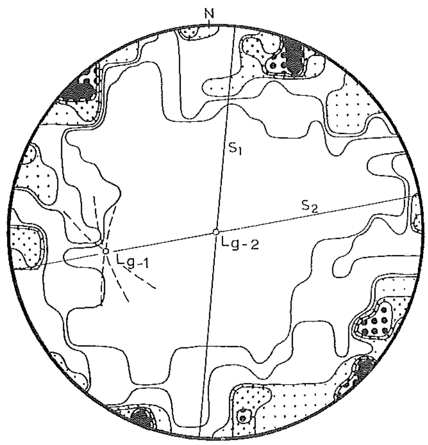

Fig. 15-i
Specimen 10, 103 cleavage poles of muscovite from the Ōtagiri granite
Contours 7–5–4–3–2–1%.

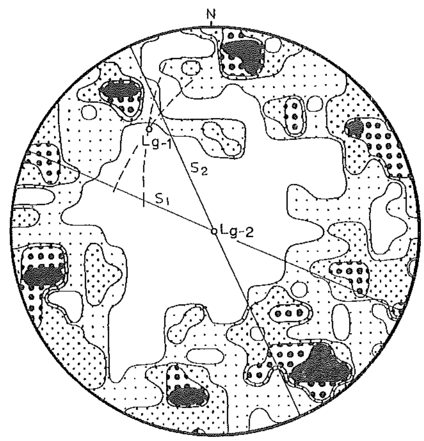

Fig. 15-j
Specimen 11, 107 cleavage poles of muscovite from the Ōtagiri granite
Contours 4–3–2–1%.

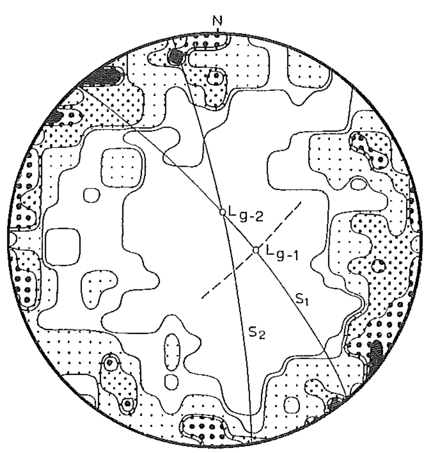

Fig. 15-k
Specimen 12, 156 cleavage poles of muscovite from the Ōtagiri granite
Contours 4–3–2.5–1–1.5%.

are characterized by monoclinic symmetry. They exhibit respectively incomplete *ac*-peripheral girdle with maxima at the fabric axis *C* and define strictly *s*-surface. In a few specimens such as 5 and 9, submaxima are recognized in each *ac*-girdle and they define the lineation L_{m-2} or L_{m-3}.

The fabrics of the Ōtagiri granites, namely the third type specimens 10, 11 and 12 (Figs. 14-j, 14-k and 14-l) is characterized by triclinic symmetry, so that the intersections of great circles corresponding to maxima and submaxima in each fabric diagram suggest the existence of two kinds of lineation in each fabric, which are denominated as L_{g-1} and L_{g-2}. These features are characteristic to the biotite fabrics of the Ōtagiri granites.

ii) The muscovite fabrics are classified into two types on the basis of girdle pattern and symmetry. Since the symmetry of the maxima in the muscovite orientation is generally dispersed than that of the biotite, the muscovite fabrics show an *ac*-peripheral girdle in the metamorphic rocks except the specimen 1 (Fig. 15-a). Such pattern is more distinct in the Ōtagiri granites.

The first type is the fabrics of specimens 1, 2, 3, 4 and 7 (Figs. 15-a, 15-b, 15-c, 15-d and 15-g) which are characterized by approximate monoclinic symmetry and partial *ac*-girdle. In each fabric of specimens 1, 4 and 7, maxima are at the fabric axes *C* and coincide with biotite maxima of each corresponding fabric. While in fabrics of specimens 2 and 3, maxima do not coincide with biotite maxima of each corresponding fabrics.

The second type is the fabrics of specimens 5, 6, 8, 10, 11 and 12 (Figs. 15-e, 15-f, 15-h, 15-i, 15-j and 15-k). It is characteristic that they hold complete *ac*-peripheral girdle and approximate monoclinic symmetry. Maxima and submaxima do not generally coincide with fabric axes *C* and also with those of biotite fabrics. When compared with the corresponding biotite fabrics, the most remarkable point in the muscovite fabrics of the Ōtagiri granites is that no correlation is found between the lineation L_{g-1} and the muscovite fabrics, although the muscovite orientation is closely correlated with the lineation L_{g-2}.

Discussion

In the biotite fabrics of the metamorphic rocks, the classification of the fabric types can be made, regardless to those of the subareas and rock species, and there is no essential difference between the fabric types. Each biotite fabric can be generally correlated well with each corresponding quartz fabric, showing more or less the tendency to form an *ac*-girdle, and the maxima define clearly *s*-surface. Since the *ac*-girdle signifies the external rotation of biotite blades about fabric axis *B*, it is clear that the biotite fabrics were yielded by comparatively simple tectonic movement which was probably involved in the up-swelling of the Ōtagiri dome, from the fact that the biotite fabrics are well correlated with the quartz fabrics.

Probably, conspicuous *ac*-girdle of the fabric specimen 5 (Fig. 14-e) may represent the influence of the granite sheet intrusion.

While the fabric patterns of biotite orientation are not so simple in the Ōtagiri granites, as those in the metamorphic rocks, suggesting the complicated movements in themselves. It is interesting that the existence of two lineations; L_{g-1} and L_{g-2} was confirmed, and also the lineation L_{g-2} is correlated with the lineation of the metamorphic rocks in subarea III as stated above. The lineation L_{g-1} may be a *b*-lineation modified by the later movement, although there still remain some problems.

Muscovite blades are subordinate to those of biotite, and it seems that the muscovite has crystallized at the same time with the biotite, as muscovite over-crosses the biotite flake and *vice versa*. Compared with the biotite fabrics, the muscovite fabrics represent a notable tendency to show *ac*-girdle. In the metamorphic rocks its symmetry is the same as that of the biotite fabrics, while in the Ōtagiri granites it differs from that of the biotite fabrics, exhibiting approximately monoclinic symmetry. The maximum positions of the muscovite fabrics of specimens 2, 3, 5, 6, 8, 10, 11 and 12 (Figs. 15-b, 15-c, 15-f, 15-h, 15-i, 15-j and 15-k) do not coincide with those of the biotite fabrics. According to CRAMPOTON (1958), biotite can be more promptly reoriented than muscovite. However, more detailed analysis is necessary for the discussion on the diversity of both maxima in question.

In the muscovite fabric of specimen 3 (Fig. 15-c), the orientations of poikiloblastic muscovites are plotted with dotts, which reveal rather random orientation. Such poikiloblastic muscovite crystals may signify a postkinematic mineralization.

Discussion and conclusion

The process of the formation of the Ōtagiri dome revealed through the megascopic and microscopic petrofabric analysis may be summarized as follows.

i) In the pre-metamorphic phase, some considerable deformation of the Paleozoic formations took place, as confirmed by the following facts; a) the speciments are found of which foliation is developed obliquely crossing the folded stratification, b) the Koyashiki fault had been activated before the metamorphism took place.

ii) The regional metamorphism, that is, the Ryōke metamorphism occurred in the following phase. The Paleozoic formations were converted to the metamorphic rocks with various grades which constituted the four metamorphic zones ranging from biotite slate zone to banded gneiss zone. With the progress of the metamorphism the subareas II, III and IV began to upheave, resulting finally in the formation of a dome. At that time, the Koyashiki fault probably played a role as the boundary line between the doming area and the non-doming area. Therefore it is clear that the Koyashiki fault was a significant tectonic line of the region in the early phase of the upheaval.

iii) From the shape of the dome and the lineation L_{m-1}, it may be presumed that the dome, in the early phase, moved upwards from south to north, resulting in a fire-ball shape.

iv) Then the dome changed the direction of its movement and became to swell upwards, having its centre in the subarea III. The present features of the megascopic structures, such as foliation S and lineation L_{m-2}, and the original patterns of microfabrics were formed through the swelling up of the dome. With the progress of the metamorphism and doming up, the dome began to form two units with somewhat different character, i.e., the inner zone and the outer zone, which were later separated by the Ōtagiri fault.

v) At the phase of the swelling, the Ōtagiri granites which had been produced by the metamorphism in the depth, migrated upwards into the centre of the dome, and intruded along the Ōtagiri fault activated simultaneously. These granites intruded forming various sheets and dykes only in the area to the south of the Ōtagiri fault. These facts suggest the structural significance of the Ōtagiri fault. The previously formed megascopic and microscopic fabrics of the subarea III were modified somewhat by the intrusion of the Ōtagiri granites and yielded the lineation L_{m-3}.

vi) Even after the intrusion of the granites, the swelling up of the dome still continued and then the orientation of the lineations L_{m-2} and L_{m-3} indicated an arched from with its axis approximately lying on the line between Kitawari and Okkoshi.

vii) The swelling of the Ōtagiri dome was followed by the intrusion of the Kisokoma granodiorite at the western side of the dome, giving thermal metamorphism to the surrounding areas. Subsequently, the Koyashiki fault was reactivated, and the Komagane fault and the Nakatagiri fault, both with the N-S trends was traversed the dome area.

The Akagi granodiorite intruded along the Komagane fault.

The eastern part of the dome in the subarea III was overlain by the Tenryū gravel.

By reviewing the sequence of the doming up of the region, it is proved that the present features of the megascopic and microscopic fabrics were formed by the deformation that was involved in the up-swelling of the Ōtagiri dome accompanied with the intrusion of the Ōtagiri granites.

It may be safely remarked that the dome had already been separated into the two units with different characters by the Ōtagiri fault when the Ōtagiri granites began to intrude, and thereafter the differences of the both units became more definite through their intrusion.

The intrusion of the Ōtagiri granites are characterized by the following two features.

i) They intruded parallel or subparallel to the foliation of the metamorphic rocks, subsequent to the up-swelling of the dome, without affording distinct effects of metamorphism or the reconstruction of the structure of the region.

ii) Their intrusion is confined only in the area to the south of the Ōtagiri fault (subarea III), while even pegmatites or aplites derived from the Ōtagiri granites are not recognizable in the area to the north of the fault.

The existence of the lineation L_{m-3} only in the subarea III may be considered to be the influence of the intrusion of the granites.

According to NUREKI (1960), the Ryōke metamorphism in the Yanai district is divided into two phases; in the earlier phase schistose hornfelses were produced by the regional thermal metamorphism which is characterized by penetrative movement, and in the later phase banded gneisses and migmatites were formed by the subsequent metamorphism which is characterized by high temperature and high confining pressure. Here the quartz fabrics of the banded gneisses are lacking of symmetry. In the Ōtagiri region, however, these feature are never recognized, and the quartz fabrics in the banded gneisses are similar to those of the schistose hornfelses, preserving monoclinic symmetry.

In the Kasagi region, according to HARA (1962), the metamorphism took place in the earlier phase, with the formation of the metamorphic rocks of various grades varying from biotite-bearing slates to banded gneisses, and in the following phase they became to show the " dome and basin " structure owing to the intrusion of the younger granite. On the contrary, since the Ōtagiri granites intruded subsequently into the up-domed metamorphic rocks, it is concluded that the swelling of the dome was not caused directly by the emplacement of the Ōtagiri granites.

Acknowledgements

The author wishes to express his sincere thanks to Prof. KENZŌ YAGI for his kindness of reading the manuscript and giving valuable advices, and to Assist. Prof. HIDEO KOBAYASHI and the members of the " Plutonism Research Group " of Hokkaidō University for their helpful suggestions. Especially he is grateful to Dr. KŌSHIRŌ KIZAKI for his kind guidance and constructive criticism throughout the present study. He is also deeply indebted to Dr. CHEOUL WOO KIM for his constant encouragement and valuable advices, and to Miss SACHIKO IKEDA for her help in preparing the paper.

References Cited

CARAMPTON, C. B. (1958): Muscovite, biotite, and quartz fabric reorientation. *Jour. Geol.* **66,** 28–34

CLOOS, E. (1947): Tectonic transport and fabric in a Maryland granite. *Bull. Comm.*

Geol. Finland, **140,** 1–14

FAIRBAIRN, H. W. and F. CHAYES, (1949): Structural petrology of deformed rocks. *Cambridge*, 117–133

GRIGGS, D. T. and J. F. BELL, (1938): Experiments bearing on orientation of quartz in deformed rocks. *Geol. Soc. Amer. Bull.* **49,** 1723–1746

HARA, I. (1962): Studies on the structure of the Ryōke metamorphic rocks of the Kasagi district, Southwest Japan. *Jour. Sci. Hiroshima Univ., Ser. C,* **4,** 163–224

ISOMI, H. and M. KATADA, (1959): Consideration on some sedimentary features of non-metamorphosed Upper Paleozoics and Ryōke metamorphics in the northern part of Kiso mountainland, Central Japan. *Bull. Geol. Surv. Japan,* **10,** 1037–1052 (in Japanese)

KASUGAI, A. (1957): Tectonic investigation on the Toyonidake migmatite dome and its neighbourhood, part 2. *Jour. Geol. Soc. Japan,* **744,** 527–540 (in Japanese)

KATADA, M. et al. (1961): Geology of Japanese Central Alps and its western area. (3) Geologic structure of Ryōke Zone. *Earth Si.*, **57,** 12–23 (in Japanese)

KIZAKI, K. (1956): Petrofabrics of the Oshirabetsu Dome in the Southern Hidaka metamorphic zone, Hokkaidō, Japan. *Jour. Fac. Sci., Hokkaidō Univ., Ser.* IV, **9,** 289–317

KVALE, A. (1953): Linear structures and their relation to movement in the Caledonides of Scandinavia and Scotland. *Quart. Jonr. Geol. Soc. London,* **109,** 51–73

MURAYAMA, M. and M. KATADA, (1957): Geological map "Akaho" (1/50,000) and its explanatory text. *Geol. Surv. Japan* (in Japanese)

NUREKI, T. (1960): Structural investigation of the Ryōke metamorphic rocks of the area between Iwakuni and Yanai, Southwestern Japan. *Jour. Sci. Hiroshima Univ., Ser.* C, **3,** 69–141

ŌKI, Y. (1958): Thermally metamorphosed rocks in the northern Kiso mountain-range, Central Japan. *Jour. Gəol. Soc. Japan,* 748, 1–12 (in Japanese)

OKAMURA, Y. (1960): Structural and petrological studies on the Ryōke gneiss and granodioritic complex of the Yanai district, Southwest Japan. *Jour. Sci. Hiroshima Univ., Ser. C,* **3,** 143–214

SANDER, B. (1930): Gefügekunde der Gesteine. *Julius Springer, Vienna*

TSUCHIYA, T. (1963): The Ryōke metamorphic rocks in the eastern foot of Kisokoma-ga-take. *The graduation thesis of Hokkaidō Univ.*, 1–53 (M.S. in Japanese)

TURNER, F. J. and L. E. WEISS, (1963): Structural analysis of metamorphic tectonites. *New York,* 230–237, 425–442

(Manuscript received Sept. 10, 1965)

Explanation of Plate 7

Explanation of Plate 7

Block diagram of the Ōtagiri Dome.

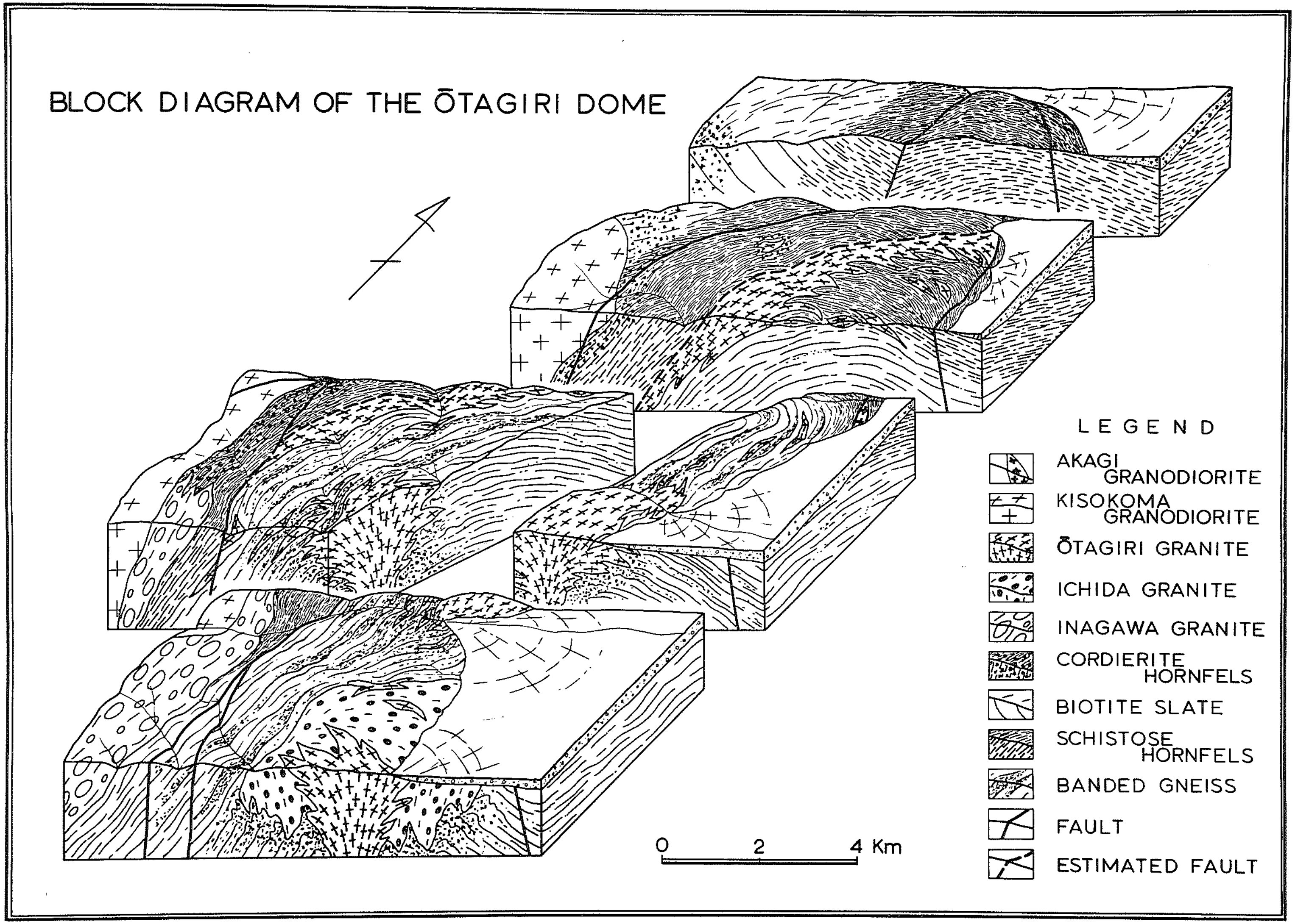
BLOCK DIAGRAM OF THE ŌTAGIRI DOME
LEGEND
AKAGI GRANODIORITE
KISOKOMA GRANODIORITE
ŌTAGIRI GRANITE
ICHIDA GRANITE
INAGAWA GRANITE
CORDIERITE HORNFELS
BIOTITE SLATE
SCHISTOSE HORNFELS
BANDED GNEISS
FAULT
ESTIMATED FAULT
0 2 4 Km

Explanation of Plate 8

Explanation of Plate 8

Tectonic map of the Ōtagiri Dome.

1. Lineation 35°> 2. Lineation 35°≦ 3. Foliation 45°> 4. Foliation 45°≦ 5. Foliation (in the Ōtagiri granites) 6. Bedding plane 7. Fault 8. Estimated fault 9. Cordierite hornfels 10. The Akagi granite 11. The Kisokoma granodiorite 12. The Ōtagiri granites 13. The Ichida granite 14. The Inagawa granite 15. The boundary line of the metamorphic zone
BS. Biotite slate **SH1**. Schistose hornfels I **SH2**. Schistose hornfels II
BGn. Banded gneiss (**I**). Subarea I (**II**). Subarea II (**III**). Subarea III
(**IV**). Subarea IV

Plate 8

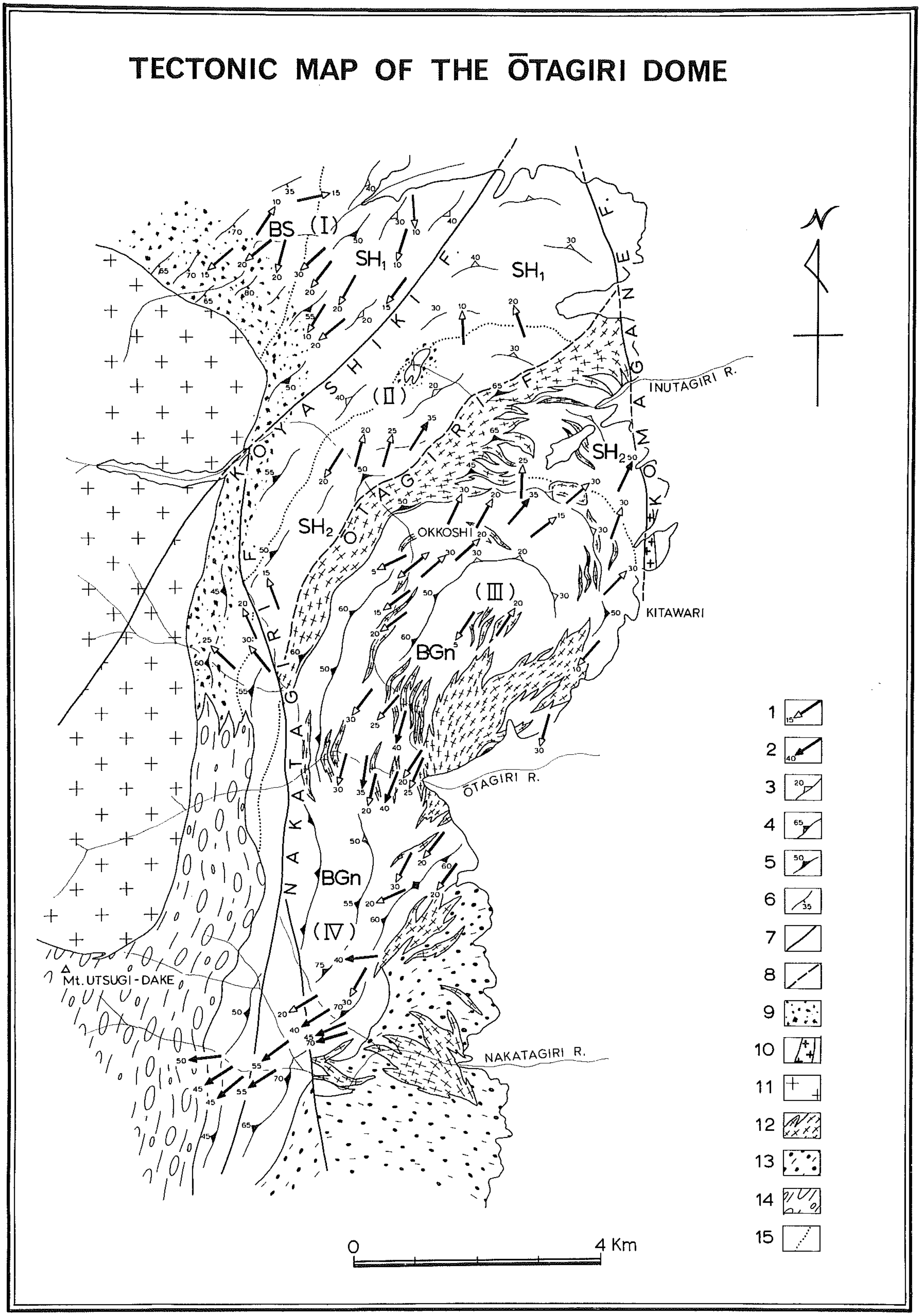
TECTONIC MAP OF THE ŌTAGIRI DOME
BS
(I)
SH1
SH1
(II)
SH2
SH2
OKKOSHI
(III)
BGn
BGn
(IV)
KOYASHIKI F.
OTAGIRI F.
NAKATAGIRI F.
KOMAGANE F.
INUTAGIRI R.
ŌTAGIRI R.
NAKATAGIRI R.
KITAWARI
Mt. UTSUGI-DAKE
0
4 Km
1
2
3
4
5
6
7
8
9
10
11
12
13
14
15